JOURNAL OF MATERIALS SCIENCE 1 (1966) 117–126

Measurement of Ionic Diffusion in Lithium Fluoride by Nuclear Magnetic Resonance Techniques

T. G. STOEBE*, R. A. HUGGINS†
Department of Materials Science, Stanford University, Stanford, California, USA

Received 11 October 1965

Rates of diffusion of ^{7}Li and ^{19}F were investigated in doped crystals of lithium fluoride using the technique of motional narrowing of nuclear magnetic resonance lines. Major doping elements were divalent Mg and Mn ions, present in amounts between 3 and 240×10^{-6} cation site fraction. Extrinsic vacancies introduced by this doping increased Li ion diffusion and caused ^{7}Li motional narrowing to begin at lower temperatures for greater impurity contents.

Diffusivities were determined from the motional narrowing curves using a method of analysis which reduces uncertainties due to magnetic field inhomogeneity and other temperature independent contributions to line broadening. Resulting log D vs $1/T$ plots showed the expected intrinsic, free vacancy extrinsic, and divalent ion-vacancy association regions of Li ion diffusivity. Activation energies determined for these regions were 1.87 ± 0.09, 0.66 ± 0.03, and 0.91 ± 0.05 eV, respectively. These values yielded the energy for motion of a cation vacancy as 0.66 eV and the energy of formation of a Schottky defect as 2.42 eV.

Experimental results obtained earlier in powdered LiF: Mn samples are clarified, and indications concerning the effects of other impurities on Li ion diffusion are presented and discussed.

1. Introduction

Nuclear magnetic resonance (NMR) techniques for the determination of diffusion parameters in alkali halide crystals have been used by a number of authors. One of these, that of motional narrowing of steady state NMR lines, has been applied in several cases [1-3], although problems with data analysis have sometimes led to results inconsistent with those of other methods. Pulsed NMR techniques have also been applied to the determination of diffusivities in such crystals [3, 4], the best example being the work of Eisenstadt in LiF [4].

In the current research, the technique of motional narrowing has been used primarily to investigate cation diffusion in LiF as a function of doping with the divalent ions Mg and Mn. LiF was used as a host material because NMR signals from both constituents could be observed, because motional narrowing occurred in a convenient temperature range, and because experimental information concerning the effects of divalent cation doping on diffusivities is not complete in this material. A data analysis technique, recently discussed elsewhere [5], was used to eliminate some of the problems faced by other investigators in the determination of diffusion parameters from their experimental results.

2. Theoretical Background

Rates of self diffusion in alkali halide crystals are dependent upon the number and type of vacancies present in the crystal lattice. Since the

*Present address: Department of Metallurgy, Imperial College, London, England.
†Present address: Max Planck Institut für physikalische Chemie, Göttingen, Germany.

addition of divalent impurities to such a crystal introduces cation vacancies to maintain charge neutrality, the investigation of cation diffusion rates can give information on defect interactions as well as vacancy mobilities.

The various regions in a plot of the temperature dependence of the diffusivity have been reviewed by Lidiard [6] and by Dreyfus and Nowick [7]. At high temperatures and in pure materials an intrinsic region is encountered, where the number of vacancies present is determined by thermal equilibrium and is independent of the presence of impurities. In this region (called region I), the cation self-diffusion coefficient D may be written as

$$D = a_0^2 \nu_0 \exp\left[(\Delta S_s/2 + \Delta S_m)/k\right] \exp\left[-(\Delta H_s/2 + \Delta H_m)/kT\right] \quad (1)$$

where ΔS_s and ΔH_s refer to the entropy and enthalpy associated with cation vacancy formation, ΔS_m and ΔH_m are the entropy and enthalpy for cation motion, and a_0 is the lattice parameter and ν_0 a frequency factor.

At lower temperatures (region II), where the number of cation vacancies is a constant governed by the divalent ion impurity content, the cation self-diffusion coefficient becomes

$$D = a_0^2 \nu_0 <V_M^-> \exp(\Delta S_m/k) \exp(-\Delta H_m/kT) \quad (2)$$

Here, the symbol $<V_M^->$ represents the site fraction of vacancies on the cation lattice (identical to mole fraction) using a notation similar to that of Kröger [8].

Reactions between vacancies and other defects can cause a decrease in the number of vacancies which are free, and thus a decrease in diffusivity from the value expected from equation 2. The most important of these effects arises from the association of impurity ions with vacancies, which attract one another due to their opposite effective charges. The consideration of the variation in the fraction of associated pairs as a function of impurity content, binding energy, and temperature, shows that almost-complete association occurs at low temperatures, with dissociation occurring most rapidly for lower impurity contents and smaller binding energies as the temperatures increase [6, 9].

The impurity-vacancy association reaction has a large effect on the temperature dependence of diffusion. Defining a quantity $<F> = <F_M^+> + <FV>$ as the overall fraction of metal ions in the system, where $<F_M^+>$ and $<FV>$ are the site fractions of divalent metal ions and divalent impurity-vacancy pairs, the site fraction of negatively-charged free vacancies $<V_M^->$ is calculated to obey [7]

$$<V_M^->^2 = (<F>/12)\exp(-\Delta G_a/kT) \quad (3)$$

in the limit of $<V_M^-> \ll <F>$. Here, ΔG_a is the free energy of association. The contribution to D of free vacancies thus becomes

$$D = a_0^2 \nu_0 \left[\frac{<F>}{12}\right]^{\frac{1}{2}} \exp\left[(\Delta S_m + \Delta S_a/2)/k\right] \exp\left[-(\Delta H_m + \Delta H_a/2)/kT\right] \quad (4)$$

where the relation $\Delta G_a = \Delta H_a - T\Delta S_a$ has been substituted.

This free vacancy contribution to diffusivity gives rise to the ionic conductivity behaviour at low temperatures which is termed region III. The actual self-diffusion coefficient in region III contains contributions due to associated vacancy motion, and more accurate diffusion relationships have been discussed elsewhere for this case [10].

The relative positions of regions I, II, and III are shown on a schematic plot of log D vs $1/T$ in fig. 1. This figure also illustrates the influence of changes in doping level on diffusivities. The activation energies, Q, for regions I and II of these curves are taken from equations 1 and 2.

The application of motional narrowing to the determination of diffusivities in an alkali halide system may be approached using the theory of Eisenstadt and Redfield [11]. Here, the dependence of the spin-spin interaction time T_2 on temperature is calculated for a system containing two species of nuclear spin. The angular dependence of the nuclear relaxation is also taken into account. The result for the main H_0 magnetic field parallel to the [100] direction in the crystal is

$$\frac{1}{T_2}(^7\mathrm{Li}) = 5.97 \times 10^8 \frac{1}{\nu_{Li}} + 3.09 \times 10^9 \frac{1}{\nu_{Li} + \nu_F} \quad (5)$$

and for H_0 parallel to the [110] direction in the crystal, the result is

$$\frac{1}{T_2}(^7\mathrm{Li}) = 1.14 \times 10^8 \frac{1}{\nu_{Li}} + 1.07 \times 10^9 \frac{1}{\nu_{Li} + \nu_F} \quad (6)$$

These results are given in terms of the jump

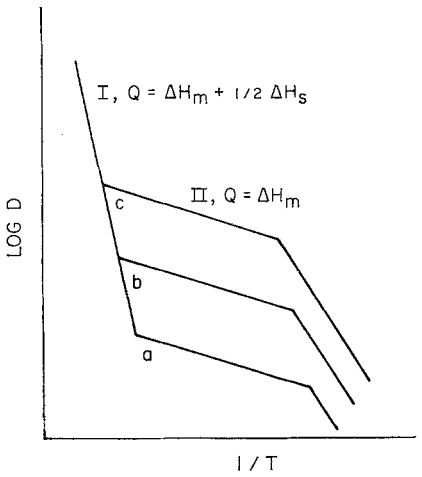

Figure 1 Typical plot of log D vs $1/T$ showing regions I, II and III, their slopes, and the effect of doping on their positions. Doping level increases for curves *a* through *c*.

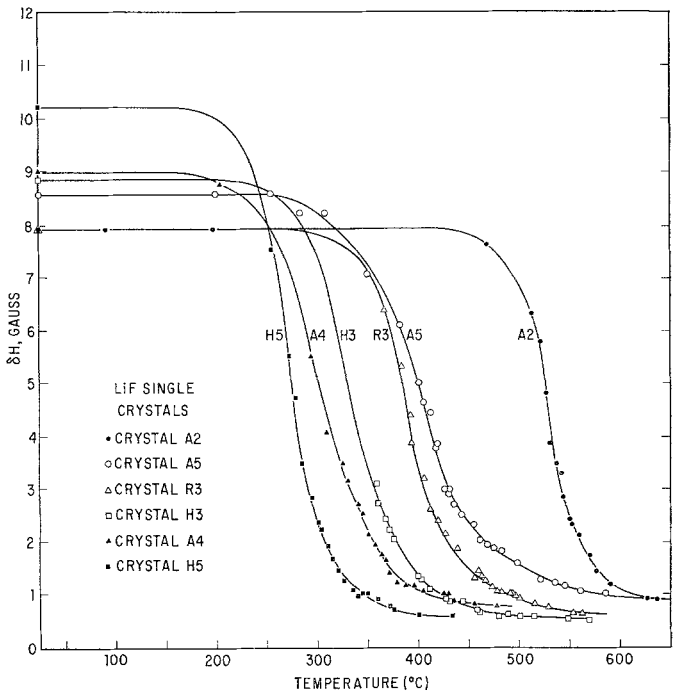

Figure 2 ^{7}Li motional narrowing curves for a series of doped LiF single crystals. Major impurity contents for these crystals are given in table I.

frequencies of Li and F ions in LiF. The steady state dipolar NMR line width δH_d is related to $1/T_2$ by the relation

$$\delta H_d = \frac{2}{\sqrt{3}} \frac{1}{\gamma T_2} \text{gauss} \qquad (7)$$

where γ is the nuclear gyromagnetic ratio. Each jump frequency is related to a diffusivity through the equation [12]

$$1/\nu = a_0^2/12D \qquad (8)$$

where the jump distance $d = a_0/\sqrt{2}$. Equations 5 and 6 have been corrected for the effect of jump correlations on free vacancy diffusion which have been discussed elsewhere [4, 10]. Therefore, D values reported here represent true macroscopic diffusion coefficients.

Since motional narrowing can be said to occur when a given rate of motion occurs, or when the diffusivity reaches a certain value, consideration of fig. 1 shows that narrowing should occur at lower temperatures for increased divalent cation doping. It should also be possible, by determining the activation energy and the pre-exponential factor for a given motional narrowing curve, to construct a portion of the log D vs $1/T$ curve for a particular system. This will be done for the Mg- and Mn-doped LiF results in the present paper.

3. Experimental Considerations

The nuclear magnetic resonance spectrometer system used in these experiments has been discussed elsewhere [5, 13]. It is capable of attaining sample temperatures up to 650° C using dry N_2 as a heating gas. Line widths are reported as the separation (in gauss) between points of maximum and minimum slope on the absorption signal.

Single crystals of LiF were grown from the melt using the Kyropoulos method [14]. The melt was doped with MgF_2 as desired to produce doped crystals. Crystal growth was performed in an argon atmosphere using a nickel crucible. Dislocation densities in these crystals were determined by etch pit techniques, yielding densities in the range 1 to 10 $\times$ $10^6/cm^2$.

A number of crystals were produced and coded according to the source of the starting material: H for Harshaw crystals, R for Baker

and Adamson reagent grade material, and A for American Fluoride high purity LiF powder; crystals of different dopings are denoted by numbers. Crystals A5 and A6 were doped with MnF_2. The amounts of dopant added to the melt for various crystals, as well as the resultant crystal dopant contents, as determined by spectrographic analysis, are shown in table I.

TABLE I Doping levels of crystals as determined by spectrographic analysis (site fraction $\times 10^6$).

Crystal	Addition to melt	Doping contents Mg	Mn
A1	none	5	
A2	none	3	
A4	200 Mg	160	
A5	500 Mn	7	13
A6	100 Mn	3	6
H2	used as rec'd	10	
H3	none	104	
H5	300 Mg	240	
H6	none	7	
R3	none	65	

The impurity contents of the H series crystals were low unless intentional doping occurred, except for crystal H3, from a different batch.

The crystals were grown in the cube orientation, seeded with a small crystal whose [100] direction was perpendicular to the surface of the melt. The grown crystals were from 25 to 75 mm in length, and up to 25 mm in diameter. Samples about 6 mm square by 18 mm long were cleaved from them using techniques discussed by Gilman and Johnston [15].

LiF powders doped with Mn were prepared at room temperature by precipitation with NH_4F from an aqueous solution of LiCl containing known amounts of $MnCl_2$. They were subsequently filtered, washed, and then dried at 100° C for a short time. Resultant LiF particles were about 25 μm diameter.

Several batches of powdered samples were prepared, both undoped, and with doping levels of 10^{-3}, 2×10^{-4}, and 4×10^{-5} cation site fraction Mn. Activation analysis showed that these dopings were indeed present in the resulting precipitate at the lower dopings, decreasing to about 80% of the desired doping at 10^{-3} site fraction. Chang *et al* [16, 17] performed electron spin resonance experiments on material prepared in essentially the same manner, and showed that the fraction of homogeneously distributed Mn decreases with increasing concentration at higher doping levels. Thus it appears that after preparation the desired concentration of Mn is present in solution in the powder, except at the 10^{-3} site fraction level, where perhaps only 5×10^{-4} site fraction is in solution.

4. Results and Discussion

4.1. Li Ion Diffusion in Mg- and Mn-doped LiF Single Crystals

^{7}Li nuclear magnetic resonance line widths were measured as a function of temperature in the Mg- and Mn-doped LiF crystals described in the previous section. The resultant motional narrowing curves for a representative set of samples are shown in fig. 2. Each point was determined as the average of several trials at a given temperature. The possible experimental errors in each point lead to an experimental uncertainty of about $\pm 8\%$ in the line width. All of these motional narrowing curves were determined with the H_0 magnetic field parallel to the [110] direction in the crystal lattice. These curves were quite reproducible, and reruns on different days showed no difficulties in the temperature measurement or angular alignment due to remounting the samples.

These motional narrowing curves illustrate that narrowing occurs at lower temperatures, and the diffusion becomes more rapid, as the divalent ion impurity content increases. The results of the data analysis show that the narrowing curve of crystal A2 is characteristic of diffusion in the intrinsic region while that of crystal A5 is in the free vacancy extrinsic region, and those of crystals R3, H3, A4 and H5 are in the divalent ion-vacancy association region of diffusivity. This transition from intrinsic to free-vacancy extrinsic and association regions can be seen qualitatively from the relative shapes of the narrowing curves; the curve for A2 is steep, indicating a high Q process, while that for A5 has a much more shallow slope corresponding to a low Q process and the other curves are intermediate in steepness.

Since some observations have been made which indicate that dislocations can influence cation diffusion, experiments were performed on some of the above crystals to observe any changes in motional narrowing caused by the presence of dislocations. Dislocations were introduced by deformation, with 10% deformation increasing the dislocation density to

$10^8/cm^2$, in agreement with the work of Gilman and Johnston [15]. No systematic changes in the motional narrowing curves were observed in these deformed crystals; as a result, dislocation effects will be ignored.

The motional narrowing curve for Mn-doped crystal A5 is the only one observed which is characteristic of extrinsic diffusion over the whole temperature range analysed. The other Mn-doped crystal, A6, containing less divalent impurity, had a narrowing curve with a higher narrowing temperature. This curve, however, seemed to be in the transition region between regions I and II. No crystals with higher Mn content could be produced because of its low solubility.

Two Mg-doped crystals, H2 and H6, were also observed to have narrowing curves in the transition region between extrinsic and intrinsic diffusivities. The analysis of such curves will be discussed later.

The room temperature line widths in the crystals shown in fig. 2 are seen to increase with increasing impurity content. This is not an orientation effect because care was taken to align H_0 with the [1 1 0] direction in the crystal lattice in all cases. Therefore, it must be due to quadupolar broadening caused by the interaction of the ^{7}Li nuclear quadupole moment with electric field gradients set up by the impurity ions. Unfortunately, it is not possible to derive quantitative information from these results, due to the relatively large experimental uncertainty in these broad room temperature lines.

The dimensions of samples used in the determination of the motional narrowing curves varied greatly, causing changes in the magnetic field inhomogeneity from sample to sample. Since the magnetic field inhomogeneity is the major factor which determines high temperature line widths, it is expected that the line width would approach a greater value in a large crystal than in a small one. This is illustrated in fig. 2, where crystals A2 and A5 were large in cross-sectional area, while the other crystals were smaller. The line width at high temperature for the largest samples was about 0.85 gauss. This is larger than the measured field inhomogeneity of 0.75 gauss, and may indicate the presence of some additional broadening mechanism such as has been observed in metallic aluminium and copper [5, 18, 19].

The shapes of these resonance lines were generally Gaussian at low temperatures, becoming nearly Lorentzian in the narrowed region. The line shape transition generally began when the line had narrowed to $\frac{3}{4}$ of its room temperature width, and was completed to within experimental error before it had narrowed to $\frac{1}{2}$ of its room temperature width.

The room temperature angular variation of the ^{7}Li NMR line width was measured in several of the crystals investigated, with the results in good agreement with theoretical calculations. An angular dependence similar to that for the room temperature lines was found to hold during narrowing, in agreement with the Eisenstadt-Redfield theory for nuclear spin relaxation.

The ^{7}Li motional narrowing curves presented above have been analysed using methods discussed in detail elsewhere [5], based on the equation

$$\delta H_m = A \exp(Q/kT) + \delta H_x \qquad (9)$$

where the dipolar line width δH_d has been written as $A \exp(Q/kT)$. Here, δH_x is a constant related to the non-dipolar broadening present, and δH_m is the measured line width. Both computer and graphical methods have been used for the solution of equation 9, with the results of the two methods being in very good agreement. In order to keep only a single exponential in equation 9, the assumption has been made that ν_F is negligible compared to ν_{Li} (i.e. $D_{Li} \gg D_F$). This assumption is valid in the extrinsic regions, since the introduction of cation vacancies considerably reduces the equilibrium number of anion vacancies, but is not valid in the intrinsic region, as will be discussed later.

Using this assumption that $\nu_{Li} \gg \nu_F$, the constant A in equation 9 may be determined in terms of D_0. The result for H_0 parallel to [1 0 0] is

$$A = 5.60 \times 10^{-11}/D_0 \qquad (10)$$

and for H_0 parallel to [1 1 0] is

$$A = 2.71 \times 10^{-11}/D_0 \qquad (11)$$

where A is in gauss and D_0 in cm^2/sec. The resulting values of the parameters A, D_0, Q, and δH_x for the motional narrowing curves shown above are given in table II. All crystals were measured with the H_0 magnetic field parallel to the [1 1 0] direction, with the exception of A1 where H_0 was parallel to the [1 0 0] direction in the crystal lattice.

Using these values of D_0 and Q, conventional log D vs $1/T$ plots may be made in order to compare the data further. Fig. 3 shows such a plot for the crystals whose motional narrowing curves have been shown in fig. 2. Using D_0 and Q values from table II, solid lines have been drawn in the temperature interval covered by the part of the motional narrowing curve which was analysed. This is generally the region where the line was narrowed to less than $\frac{1}{2}$ of the room temperature width. It can be seen that motional narrowing studies of ^{7}Li in LiF can only be used to determine Li ion diffusivities in the region between about 10^{-11} and 3×10^{-10} cm^2/sec. However, the large differences in slope observed in this region for different impurity contents illustrate that it is nevertheless possible to obtain significant information about diffusion mech-

TABLE II Results of data analysis

Crystal	A (gauss)	D_0 (cm^2/sec)	Q (eV)	δH_x (gauss)
A1	6.68×10^{-12}	8.39	1.90	0.850
A2	3.62×10^{-12}	7.49	1.90	0.751
A2 (corrected for F ion motion)		4.10	1.87	
H6	5.51×10^{-9}	4.92×10^{-3}	1.35	0.591
H2	9.13×10^{-7}	2.97×10^{-5}	0.95	0.400
A5	3.97×10^{-5}	6.82×10^{-7}	0.66	0.665
R3	3.29×10^{-7}	8.23×10^{-5}	0.93	0.483
H3	2.48×10^{-7}	1.09×10^{-4}	0.88	0.391
A4	8.64×10^{-8}	3.14×10^{-4}	0.89	0.633
H5	1.54×10^{-8}	1.76×10^{-3}	0.92	0.477

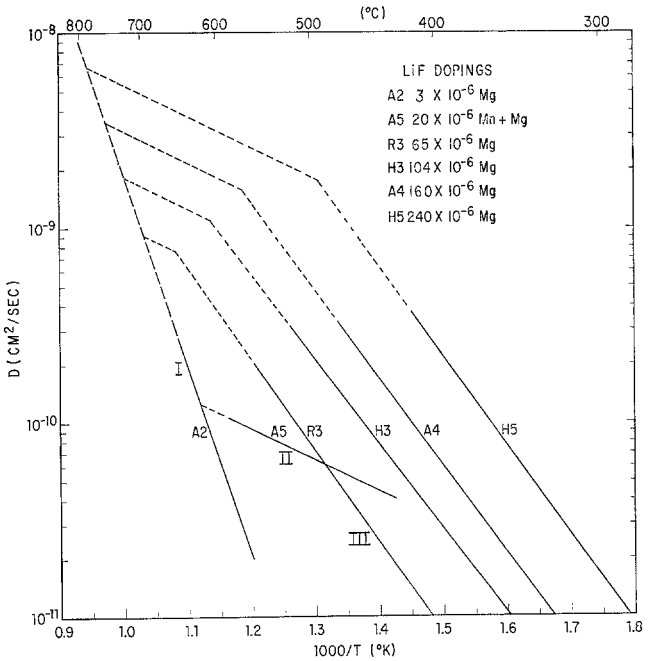

Figure 3 Log D vs $1/T$ plot for the crystals whose motional narrowing curves were shown in fig. 2, determined as described in the text.

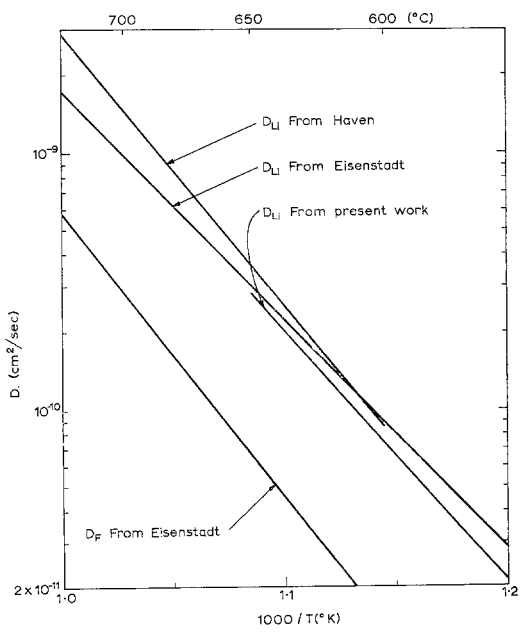

Figure 4 Log D vs $1/T$ plot for ^{7}Li diffusion in crystals A2, corrected for F in motion, compared with data from the literature. Haven's data were obtained from conductivity measurements and Eisenstadt used pulsed NMR techniques.

anisms and defect interactions from such motional narrowing studies.

The curves shown in fig. 3 are characterised by three different slopes, generally corresponding to the intrinsic, free vacancy extrinsic and divalent ion-vacancy association regions as discussed previously. Narrowing curves in the intrinsic region yielded nearly identical D values despite differences in impurity contents. This is as it should be for the case of a true intrinsic region.

The work of Eisenstadt [4] has shown that D_F is about 0.2 D_{Li} in the intrinsic diffusion region. Thus, the assumption $D_{Li} \gg D_F$ used in analysing the data is not valid in this region. The data are easily corrected for this fluorine diffusion term, however, using equations 9 and 5 or 6. This was done for the data of crystal A2, and amounted to a factor of about 0.8 in this temperature region. The corrected values for D_0 and Q have been given in table II and were used in fig. 3.

The intrinsic diffusion data obtained from this work are compared with previous experimental determinations of D_{Li} in fig. 4, where D_F is also shown for reference. The ionic conductivity data of Haven [20] were converted to diffusivity values using the Einstein relation (6) and give an activation energy of 1.99 eV. The Li ion diffusion data of Eisenstadt give an activation energy of 1.81 eV. Reasonable limits of error for the present results, due mainly to the experimental uncertainty in each data point, amount to $\pm$ 5%. Thus, the present result for the activation energy in the intrinsic region, 1.87 $\pm$ 0.09 eV, is seen to agree well with these other values. The absolute magnitudes are also in good agreement with those of the other investigators; in particular, the present results are well within the range of scatter of Eisenstadt's data.

The experimental results in the free vacancy region are limited to one motional narrowing curve in a Mn-doped single crystal (crystal A5). No free vacancy extrinsic region was observed in any of the Mg-doped crystals, presumably because Mg ions associate more readily with vacancies than do Mn ions. The experimentally determined activation energy for this region, 0.66 $\pm$ 0.03 eV, is in good agreement with the results of Haven and Eisenstadt, who obtained 0.65 and 0.72 eV, respectively.

The motional narrowing curves of the two Mg-doped crystals, H2 and H6, which appeared to be in the transition region between intrinsic and extrinsic regions, were analysed using equation 9, and the resultant diffusion parameters have been given in table II. On a log D vs $1/T$ plot, these curves also appear to be in the transition region between intrinsic and extrinsic behaviour. This illustrates a major problem with the motional narrowing technique, caused because any one curve may be analysed only in terms of a single exponential. If the curve spans a transition region between processes with different activation energies, only a composite average result is obtained, and in fact it is difficult for the computer to fit the data to equation 9 in such a case. Thus, the free vacancy extrinsic region would only be visible in Mg-doped crystals if it extended over a wider temperature range.

The activation energy in the intrinsic region can be written as $\Delta H_m + \Delta H_s/2$, as defined in equation 1. Since the activation energy in the free vacancy extrinsic region is just ΔH_m, a value of ΔH_s may be determined from the experimental data presented above. This yields $\Delta H_s = 2.42$ eV.

This value may be used to determine the temperature dependence of the equilibrium number of thermally activated Li ion vacancies in the system, $<V_{Li}^->_{eq}$. In the intrinsic region, this is given by [6]

$$<V_{Li}^->_{eq} = \exp(-\Delta G_s/2kT) = \exp(\Delta S_s/2k) \exp(-\Delta H_s/2kT) \quad (12)$$

While ΔH_s is known from experiment, the value of the constant $\exp(\Delta S_s/2k)$ must be determined by some independent calibration. This is furnished by the point of intersection of curves A2 and A5, since extrinsic and intrinsic vacancy concentrations will be equal at such a point. The divalent cation ion concentration was carefully determined in crystal A5 to be 20×10^{-6} site fraction. Taking this as the calibration point, one obtains

$$<V_{Li}^->_{eq} = 1.2 \times 10^2 \exp(-1.21/kT) \quad (13)$$

One possible source of error in this expression is the contribution of other species to Li ion diffusion in this region, as was the case in the experiments of Mapother *et al* [21]. Such a contribution would cause D to be higher than the value calculated from σ using a free vacancy model. However, Haven [20] determined from his ionic conductivity results that

$$<V_{Li}^{-}>_{eq} = 5 \times 10^{2} \exp(-1.34/kT) \quad (14)$$

Using this result for the proper impurity contents, the present values of D are slightly lower, rather than higher, than the values predicted from conductivities. Thus, it can be assumed that free vacancies are the only mode of Li ion migration in region II for crystal A5.

Using equation 13 in connexion with the known divalent ion concentrations in the Mg-doped crystals (R3, H3, A4, H5), whose log D vs $1/T$ curves have been given in fig. 3, it is possible to approximate the higher temperature portions of these curves. That is, their free vacancy extrinsic regions may be established using curves of slope 0.66 eV which intersect the intrinsic curve where

$$<V_{Li}^{-}>_{eq} = <Mg_{Li}^{+}> = 1.2 \times 10^{2} \exp(-1.21/kT) \quad (15)$$

Furthermore, the intersection of such curves with the extrapolation to higher temperatures of the observed log D vs $1/T$ curves gives the low temperature limit to region II and the high temperature limit of region III. Such a procedure thus provides the approximation to the complete log D vs $1/T$ curves expected for such crystals and is useful for comparison with other experimental results. The results of this procedure are shown in fig. 3 as dotted lines. These should be fairly accurate, except that if motion of neutral pairs occurs in region II for these Mg-doped crystals, one would expect that that portion of the actual diffusion curves would be higher than those shown.

Four curves are shown in fig. 3 which are associated with region III, the divalent ion-vacancy association region. The slopes of these curves indicate a region III activation energy of 0.91 ± 0.05 eV. While correlation effects due to the motion of associated vacancies make the interpretation of this activation energy difficult, it is probably a good approximation to the activation energy for macroscopic diffusion in this region [10]. That this value is indeed characteristic of region III was indicated by experiments on samples doped with both Mg and OH, in which precipitation occurred and a steeper slope was observed, attributable to what is generally termed region IV [7]. These experiments will be discussed in detail elsewhere [22].

While no similar NMR measurements have appeared in the literature in this region, the work of Bergé *et al* [23, 24] provides ionic conductivity measurements in LiF. Unfortunately, their crystals were doped to a higher level than any of the present crystals so that a direct comparison is not possible. However, their results indicate a region III slope of about 1.1 eV, this value being larger than that found in the present experiments, as expected from correlation considerations.

4.2. ^{7}Li Motional Narrowing in Mn-doped LiF Powders

^{7}Li NMR widths were determined as a function of temperature for the Mn-doped LiF powders whose preparation was discussed above. Motional narrowing curves for various samples in the series were almost identical, indicating an apparent lack of dependence of motional narrowing behaviour on Mn content.

The analysis of these narrowing curves was carried out using equation 9 and the Torrey relaxation theory [25]. The resultant activation energies were found to be 0.74 eV. This value is only of limited accuracy, however, due to a small number of data points.

As reported previously [26], NMR lines could not be observed in these samples between 210° C and about 350° C. This was probably caused by a loss of paramagnetic relaxation centres from the system, which caused an increased T_1 and thus an inability to observe the signal under steady state conditions. The loss of paramagnetic ions from the system by precipitation was verified using electron spin resonance studies. The electron spin resonance spectrum of the samples, as grown at room temperature, showed hyperfine and superhyperfine lines similar to those seen by Chang [16]. Samples heated to 300° C, however, showed only one broad spin resonance line, indicating the presence of precipitates. Furthermore, the powders appeared black, indicating the presence of a manganese compound at the surface, similar to that seen by Schneider and Caffyn [27] in NaCl.

This precipitation process was not reversible, as no NMR lines could be observed at room temperature after the initial heating of the sample. The kinetics of precipitation were rapid at 300° C, and no lines could be observed at that temperature, even after rapid heating. The disappearance of the line was observed dynamically once, however, after rapid heating to 225° C. The line was nearly normal at first observation (after about 2 min at temperature), but became broader and of diminished ampli-

tude during the second observation (after about 4 min), and was almost gone after about 5 min at temperature.

This observation of precipitation verifies the low solubility of Mn in LiF observed for the single crystals above. It also explains the apparent lack of dependence of motional narrowing on Mn content in these powders. It is probable that the Mn is only of minor importance in introducing cation vacancies into this system, and that other divalent impurities introduce the extrinsic cation vacancies. Such impurities could have been co-precipitated with the insoluble crystallites during preparation. The most likely ones are Ca^{++} and Mg^{++}, these being major impurities in the LiCl starting material.

4.3. Nuclear Spin-Lattice Relaxation Effects

While no steady state NMR signal is visible in very pure Harshaw LiF crystals at room temperature, the presence of paramagnetic impurities can change this drastically. The addition of a few parts per million of Fe, for instance, makes room temperature lines visible in these crystals and reduces T_1 to the point where no saturation occurs for H_1 fields of up to 0.15 gauss. Very small concentrations of paramagnetic ions were deliberately introduced during growth from the melt in many of the crystals used in this work.

A major concern in this work was the influence of the paramagnetic ions on motional narrowing, as it was very convenient from visibility considerations to introduce small amounts of such impurities into the samples. However, no effects were observed other than the spin-lattice effects described below. This is undoubtedly due to the small numbers of paramagnetic ions present; if any narrowing occurred due to the migration of the paramagnetic ions, it would have an unobservably small effect on the ^{7}Li line width.

At temperatures between room temperature and the narrowing temperature in these paramagnetic ion-doped crystals, it was observed that the resonance lines broaden. This broadening was seen in all crystals investigated except when the radiofrequency field was reduced to values of about 0.002 gauss, and occurred at higher temperatures for purer samples.

Saturation experiments indicated T_1 values as low as 5 msec at room temperature, which increased to several seconds at the point of greatest broadening. This evidence indicates that this phenomenon may be associated with either a decrease in the number of relaxation centres or a decrease in their effectiveness, giving rise to a reversible increase in T_1 with increasing temperature.

While this explanation remains to be substantiated, this effect has little influence on the motional narrowing itself, as T_1 again becomes small when motional narrowing sets in. For example, T_1 is 250 msec at the onset of narrowing (540° C) in crystal A2, reducing to 40 msec when almost fully narrowed (600° C).

4.4. Fluorine Ion Diffusivities

This line broadening phenomenon was also observed for ^{19}F nuclei in these LiF crystals. Combined with the slower diffusivity [4] of ^{19}F in LiF, this prevented the quantitative determination of F ion diffusivities. Qualitatively, however, the ^{19}F resonance narrowed at about 590° C in high purity crystal A2, while in doped crystal A3 the narrowing occurred at 650° C. This indicates slower anion motion in the doped crystal, as expected from theory.

Acknowledgements

The authors are grateful to Dr T. O. Ogurtani for many helpful discussions. The LiF crystals were grown under the direction of R. S. Feigelson and the activation analysis was performed by G. W. Martin. This work was partially supported by the US Atomic Energy Commission and by the Advanced Research Projects Agency, through the Center for Materials Research at Stanford University.

References

1. F. REIF, *Phys Rev.* **100** (1955) 1597.
2. J. ITOH, M. SATOH, and A. HIRAKI, *J. Phys. Soc. Japan* **18** (1963) Suppl. II, 57.
3. R. R. ALLEN and M. J. WEBER, *J. Chem. Phys.* **38** (1963) 2970.
4. M. EISENSTADT, *Phys. Rev.* **132** (1963) 630.
5. T. G. STOEBE, R. D. GULLIVER II, T. O. OGURTANI, and R. A. HUGGINS, *Acta Met.* **13** (1965) 701.
6. A. B. LIDIARD, *Handbuch der Physik* **20** (1957) 246.
7. R. W. DREYFUS and A. S. NOWICK, *Phys. Rev.* **126** (1962) 1367.
8. F. A. KRÖGER, "Chemistry of Imperfect Crystals" (North-Holland, Amsterdam, 1964).
9. A. B. LIDIARD, *J. Appl. Phys.* **33** (1962) 414.
10. T. G. STOEBE, T. O. OGURTANI, and R. A. HUGGINS, *Phys. Stat. Sol.* **12** (1965) 649.
11. M. EISENSTADT and A. G. REDFIELD, *Phys. Rev.* **132** (1963) 635.
12. S. CHANDRASEKHAR, *Rev. Mod. Phys.* **15** (1943) 1.

13. T. G. STOEBE, Ph.D. Dissertation, Stanford University (1965).
14. R. W. DREYFUS, "The Art and Science of Growing Crystals" (Wiley, New York, 1963), p. 410.
15. J. J. GILMAN and W. G. JOHNSTON, "Dislocations and Mechanical Properties of Crystals" (Wiley, New York, 1957), p. 116; *Solid State Physics* **13** (1962) 147.
16. T. T. CHANG, Ph.D. Thesis, University of Colorado (1962).
17. T. T. CHANG, W. H. TANTTILA, and J. S. WELLS, *J. Chem. Phys.* **39** (1963) 2453.
18. J. J. SPOKAS and C. P. SLICHTER, *Phys. Rev.* **113** (1959) 1462.
19. C. P. FLYNN and E. F. W. SEYMOUR, *Proc. Phys. Soc.* 77 (1962) 922.
20. Y. HAVEN, *Rec. Trav. Chim. Pays-Bas* **69** (1950) 1471.
21. D. MAPOTHER, H. N. CROOKS, and R. MAURER, *J. Chem. Phys.* **18** (1950) 1231.
22. T. G. STOEBE, to be published.
23. P. BERGÉ, *Bull. Soc. Franç. Min. Crist.* **83** (1960) 57.
24. M. DUBOIS, P. BERGÉ, and G. BLANC, *Disc. Faraday Soc.* **31** (1961) 167.
25. H. RESING and H. TORREY *Phys. Rev.* **131** (1963) 1102.
26. T. G. STOEBE, T. O. OGURTANI, and R. A. HUGGINS, *Phys. Rev.* **134** (1964) A963.
27. E. E. SCHNEIDER and J. E. CAFFYN, "Report on the Conference on Defects in Crystalline Solids" (Bristol, 1954; The Physical Society, London, 1955), p. 74.